DELINEATION AND VISUALIZATION OF PROSTATE CANCER FOR TARGETED RADIATION THERAPY (RT)

R. Stoyanova[1], R. Rajpara[1], E. Bossart[1], V. Casillas[2], J. Palma[1], M. Abdel-Wahab[1], and A. Pollack[1]
[1]Radiation Oncology, University of Miami, Miami, Florida, United States, [2]Diagnostic Radiology, University of Miami, Miami, Florida, United States

Introduction: The precise delineation of a tumor mass from its surrounding normal tissues would allow the delivery of a boost-dose of radiation for complete eradication of tumor cells. Dynamic Contrast-Enhanced Magnetic Resonance Imaging (DCE-MRI) significantly improves cancer detection by highlighting the areas of increased microvascularity which is characteristic for tumors[1]. Various techniques are used to analyze these curves[2,3]. In this paper, we present an alternative approach for analysis of the contrast-to-time curves, which is based on an unsupervised pattern recognition (PR) technique that captures the pixel-enhancing behavior in its entirety, during both the uptake and wash-out of the contrast, and integrates this information into the standard anatomical images.

Methods: The DCE-MRI data was acquired on a 3T MR scanner (Siemens Trio Tim, Erlangen, Germany): resolution 0.7 × 0.7 × 2.5 mm^3; field of view: 360 × 264 mm; 72 slices (no gap); 5.1 ms repetition time/2.3 ms echo time; flip angle 10°. Prior to contrast material injection, one set of MR images was acquired, followed by 11-12 post-contrast imaging datasets (37 s each). The Region of Interest (ROI) was manually outlined on each axial slice. Let $I_{i,j}$ denote the ROI on the i^{th} axial slice at j^{th} time point and let **D** be the matrix of the DCE-MRI data: $\mathbf{D}=\begin{pmatrix} I_{1,1} & \cdots & I_{1,m} \\ \vdots & \ddots & \vdots \\ I_{n,1} & \cdots & I_{n,m} \end{pmatrix}$ where *n* is the number of slices within the ROI and *m* is the number of acquired time series. Principal Component Analysis (PCA) is applied to **D** to determine *k* – the number of significant Principal Components (PCs). The data is further analyzed with the constrained non-negative matrix factorization (cNMF)[4] method, which assumes each image to be a mixture of *k* tissue components with individually associated basic contrast-to-time curves. cNMF determines representation of **D** as a product of *k* basic contrast signatures (***S***) and their weights (***W***), i.e. $\mathbf{D} \approx \boldsymbol{W} \times \boldsymbol{S}$, where $\boldsymbol{W}=\begin{pmatrix} W_{1,1} & \cdots & W_{1,k} \\ \vdots & \ddots & \vdots \\ W_{n,1} & \cdots & W_{n,k} \end{pmatrix}$ and $\boldsymbol{S}=\begin{bmatrix} S_1 \\ \vdots \\ S_k \end{bmatrix}$ under the constraint that all elements of ***W*** and ***S*** are non-negative. A major advantage of cNMF is that the identified temporal patterns have direct physical interpretation (fast, slow, constant) and thus, we can relate their corresponding weights (amplitudes, strengths) to a particular tissue. After visual inspection of the curves in ***S,*** the presence/absence of the tumor tissue's temporal signature S_T is determined. S_T is characterized by a relatively fast contrast uptake and wash-out (ref). The values of its corresponding weight W_T>**T** (threshold), where **T**=mean(W_T)+2.5stdev(W_T) is overlaid as a heat map on the corresponding T2-weighted MRI (T2-w).

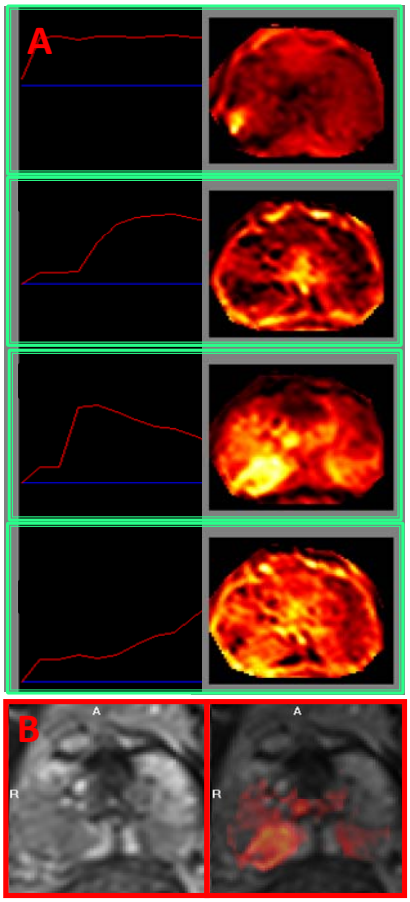

Figure 1. A. Basic signal-to-time patterns determined within the prostate in DCE-MRI studies of a patient with prostate cancer and their corresponding weights displayed as heat maps in one slice of the prostate. B. Corresponding T2-w, showing areas of hypointensity, suspicious for cancer. The same image is overlaid with the map of the tumor pattern.

Results: We identified forty six records of patients treated with RT between 6/1/08 and 6/1/09. From this cohort 25 had intact prostates and 21 were post-prostatectomy patients. The analysis of the data is ongoing; to date we have analyzed a total of 21 DCE-MRI studies. Of the six datasets analyzed for patients with intact prostates thus far, we found evidence of tumor in four. An example of the results from one of these patients is shown in Figure 1. PCA applied to ROI outlining the prostate yielded four significant PCs (*k*=4). The four curves (***S***) identified by cNMF and their corresponding strengths (***W***) are shown for one ROI slice in Figure 1A. The first curve is almost constant throughout the experiment and its spatial location indicates that it is associated with a hematoma nodule. The second and fourth patterns are related to tissues with a relatively slow contrast uptake. And lastly, the third curve depicts fast contrast uptake and wash-out, which is characteristic of tumor tissue (S_T). In Figure 1B the T2-w of the prostate from the same axial slice is presented. There is a large area of hypointenisty, mostly on the right side. The image is overlaid with the thresholded magnitude and its location coincides with the hypointensity on the T2-w. It should be noted that the analysis is carried out in all ROI slices simultaneously, resulting in tumor delineation in 3D.

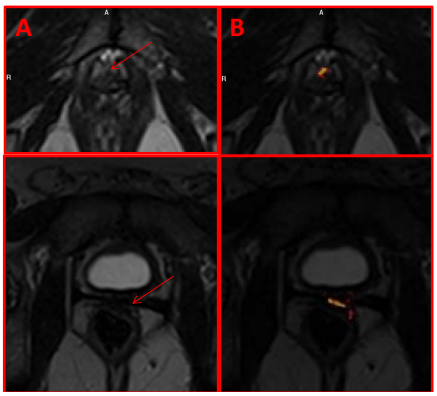

Figure 2. A. Two T2-w axial views from patient after prostatectomy. B. T2-w, overlaid with the map of the tumor pattern.

From the prostatectomy patients we have analyzed 15 datasets. Overall, eleven patients had findings suggestive of tumor as visualized by DCE-MRI. A total of 17 areas suspicious for malignancy were identified: 10 in the prostate bed; 4 in lymph nodes; and 3 in the seminal vesicle remnants. An example of the results from the post-prostatectomy DCE-MRI analysis is presented in Figure 2. In this patient we identified two separate areas suspicious for tumor. They are depicted by the map of the thresholded weights W_T on the T2-w (Figure 2B).

Conclusions: Our analysis indicates that we can detect the area of tumor burden in the prostate as well as abnormalities suggestive of residual/recurrent tumor in the prostate bed. The constructed 3D maps can be directly imported into DICOM-RT ready format to the RT planning system for targeting of the contrast enhancing areas specifically in order to improve tumor control and limit toxicity.

References: [1]Alonzi, R., A.R. Padhani, C. Allen, *Eur J Radiol,* 2007. **63**(3): p. 335-50. [2]Tofts, P.S., et al., *J Magn Reson Imaging*, 1999. **10**(3): p. 223-32. [3]Padhani, A.R. and J.E. Husband, *Clin Radiol, 2001.* **56**(8): p. 607-20. [4]Du S, Sajda P, Brown T, Stoyanova R. *Conf Proc IEEE Eng Med Biol Soc* 2005, **2**: p.1095-1098.